Undergraduate Journal of Experimental Microbiology and Immunology (UJEMI) Vol. 29:1-15

Effects of a Resistant Starch Diet on Mouse Gut Microbiome Inadequately Translates to Findings in a Human Model

Alma Garcia[1], Vincent Hsiung[2], Lina Shalaby[2], Gurpreet Sidhu[2], Kishor Sivanesan[2]

[1]Department of Genome Science and Technology, University of British Columbia, Vancouver, British Columbia, Canada
[2]Department of Microbiology and Immunology, University of British Columbia, Vancouver, British Columbia, Canada

SUMMARY Resistant starch diets are shown to provide various health benefits in humans due to the production of short-chain fatty acids from the gut microbiota. However, there is still ongoing debate on how to effectively study the effects of resistant starch consumption on human metabolism and body functions. While animal models, particularly mice, offer useful insights into biological processes and allow for controlled experiments, their relevance to human physiology and disease susceptibility is oftentimes challenged. This study compares the impact of a resistant starch diet on gut microbiome composition and function between human and humanized mouse models to determine the acceptability of mouse models for comparative analysis with humans. Using datasets from a human and humanized mouse study, significant differences were observed in both alpha and beta diversity metrics, indicating distinct microbial composition between human and mouse cohorts. Additionally, few shared taxa were found among all groups, indicating notable differences in microbial composition. Differential abundance analysis further highlighted significant differences between human and mouse groups, while PICRUSt2 analysis indicated divergent gut microbiome functions between the human and mouse model. Overall, these findings suggest that the humanized mouse model may not adequately represent the gut microbiome response to resistant starch diet observed in humans, emphasizing the need for cautious interpretation and investigation when extrapolating animal model results to human health contexts.

INTRODUCTION

Starch is a widely consumed carbohydrate in human diets and is composed of amylose and amylopectin polymers (1). In particular, resistant starches are those that resist digestion due to the human digestive enzyme's inability to break down the starch polymers (1,2). There are four types of resistant starches (Type 1, Type 2, Type 3, and Type 4) and these types are differentiated based on their structural (1). As a result of their inability to be digested, resistant starches are fermented by resident gut microbiota in the large intestine (1). This bacterial fermentation process selects for the increase of short-chain fatty acid producing bacteria in the large intestine (1). These short-chain fatty acids (SCFAs), such as acetate, propionate, and butyrate, affect glucose homeostasis, inflammation, and satiety (1). Decreased production of these SCFAs, characterized as gut dysbiosis, can result in decreased immunity and resilience to certain non-communicable diseases such as inflammatory bowel disease (IBD), type 1 and type 2 diabetes, and cardiovascular disease (2,3). Studies have also shown that RS2-rich diets can attenuate acute postprandial glucose and insulin responses, total serum cholesterol, and low-density cholesterol, thus illustrating the positive impact a RS-rich diet can have on preventing chronic diseases like type 1 and type 2 diabetes (1,2).

In order to investigate how a Resistant starch type-2 (RS2) enriched diet can alter the human gut microbiome composition, Hughes et al. (2021) conducted a randomized, placebo-controlled trial investigating the effects of RS2-enriched wheat on glycemic response and the gut microbiota. They were able to find that RS2-enriched wheat is associated with a decrease in alpha diversity and increases in starch-degrading bacteria like *Bifidobacterium, Ruminococcus, Roseburia,* and *Faecalibacterium* (2). Bendiks et al. (2020) also investigated the responses of the gut microbiome in 13 human RS2 intervention studies (1). The outcomes of their study included reductions in bacterial alpha diversity, increased production of short-chain fatty acids (SCFAs), and the enrichment of *Ruminococcus bromine, Bifidobacterium adolescentis* gut taxa (1). They noted that the subset of gut taxa that can metabolize RS2 and produce SCFAs became enriched in the gut microbiome (1).

Published Online: September 2024

Citation: Garcia, Hsiung, Shalaby, Sidhu, Sivanesan. 2024. Effects of a resistant starch diet on mouse gut microbiome inadequately translates to findings in a human model. UJEMI 29:1-15

Editor: Shruti Sandilya and Ronja Kothe, University of British Columbia

Address correspondence to:
https://jemi.microbiology.ubc.ca/

Similar research has been done to investigate the effect of a RS-rich diet on the mouse gut microbiome. Kadyan et al. (2023) investigated the effects of dietary pulses-derived resistant starch on gut microbiome in mice carrying a human microbiome. They observed differential abundance of SCFAs, such as butyrate and propionate, in mice after treatment with an RS-rich diet (3). They also concluded that the increase in SCFA production can be explained by the increase in *Firmicutes* and *Bacteroidota* in the mice gut microbiome after exposure to an RS-rich diet, reinforcing that an RS-rich diet does indeed alter the gut microbiome composition of mice (3).

Nguyen et al. (2015) studied the translatability of mouse gut microbiome changes to humans by looking at the compositional changes based on diet and disease. They found that since mouse diets are easier to control in a lab, gut microbiome changes may differ slightly between mice and humans, but if both diets are fairly consistent, the alterations in the gut microbiota are similar (4). These diets are usually standardized chow diets, so little is known about what changes exist between human and mouse gut microbiome after being given an RS-rich diet (4). Based on the current body of knowledge, there is evidence to suggest that the mouse model will exhibit similar changes in their gut microbiome composition relative to the human model when given a resistant starch diet. It is important to also note that mice are coprophagic (feces-eating species) and the large bowel differs from humans, pigs, and dogs (5). Thus, this can contribute to potential differences between human and mouse models. However, since the mouse dataset in the study by Kadyan et al. (2023) uses humanized mice, the researchers can better simulate human conditions and potentially bridge the gap between traditional mouse models and human physiology, offering valuable insight into the effects of a RS-rich diet in microbiome composition.

Mouse and human gut microbiomes have shown compositional changes after an increase in resistant starch in the diet. Even with this research, there is still much more to learn about the effects of an RS diet on the gut microbiome. Little is known about the similarities between how an RS diet affects human and mouse gut microbiome, and we strive to investigate if using a mouse gut microbiome serves as an adequate model and predictor of the effect of RS diet on the human gut microbiome. Therefore, there remains a gap in our knowledge regarding the translatability of findings from animal models to humans, particularly in the context of dietary interventions, such as the RS diet. To address this gap, we investigate how a RS diet affects the gut microbiome composition between mouse and human models, while evaluating the acceptability of a mouse model for comparative analysis with humans. In order to answer this research inquiry we performed alpha and beta diversity metrics, core microbiome, differential abundance, indicator taxa and PICRUSt2 analyses on the collected datasets to determine whether the change in gut microbiome composition in mice before and after RS is synonymous to the change in gut microbiome composition in humans before and after RS. Our research question arises from the growing interest in understanding the role of diet in shaping the gut microbiome and its overall implications on human health.

We hypothesize that this RS dietary shift will play a role in shaping the composition of the gut microbiome in both mice and humans in a similar manner, and consequently favoring specific taxa and microbial species that are different from a non-resistant starch diet. This hypothesis is grounded in previous research suggesting that dietary interventions, such as the implementation of a RS diet, can significantly impact the gut microbiome composition in both mice and humans (1,2). Drawing from existing knowledge, mouse models are one of the most commonly used models for human comparisons, as they have a considerable overlap in their genetic makeup with humans, with protein-coding regions having on average approximately 85% similarity, varying between 60% and 99% (6). As a result, by comparing the responses of mouse and human models to RS diets, we aim to investigate the degree of similarity in gut microbiome changes induced by this dietary intervention across species.

The motivation behind this research is to help bridge the gap between animal studies and human applications in the field of gut microbiome research. While animal models, particularly mice, offer valuable insights into biological processes and enable controlled experiments, their relevance to human physiology and disease susceptibility is often questioned (6). Therefore, understanding the extent of which findings from mouse models can be extrapolated to humans is essential for translating preclinical research findings into effective clinical applications. By revealing the similarities and differences in gut microbiome

responses to RS diets between mouse and human models, this study provides new insight that can inform the design of future studies focused on modulating the gut microbiome for improved human health.

METHODS AND MATERIALS

Human dataset. The human dataset was generated by Hughes et al., who analyzed the effects of resistant starch on the gut microbiome in 30 healthy individuals, aged 40-65 years old using a double-blind, randomized, placebo-controlled, crossover trial (2). For the first arm of the trial, participants were assigned to either a resistant starch enriched diet (containing 14-19g of resistant starch) or a wild type (control) diet (containing 2-3g of resistant starch) for a week. This was followed by a two-week washout period to reset the gut microbiome, before commencing the second arm of the trial where participants' diet was switched for another week (2). Fecal samples were collected prior to the beginning of each treatment, as well as at the end of each weeklong treatment (2). After DNA collection from the fecal samples, the V3 and V4 regions of the 16S rRNA gene were amplified to produce 120 samples from 30 individuals at 4 time points: prior to and after the first treatment of the trial, and prior to and after the second treatment of the trial (2). For our analysis, we used the samples after the treatment, for a total of 30 human RS samples and 30 human control samples.

Mouse dataset. The mouse dataset was generated by Kadyan et al., who looked at the effects of RS2 on the gut microbiome in mice with a humanized gut microbiome (3). The researchers depleted the mice of their gut microbiome and transplanted a pooled fecal sample from five individuals aged 50-55 into the depleted mice (3). These mice with humanized microbiomes were randomized into 3 groups: control diet, enriched resistant starch diet (using one of four different sources: pinto beans, black-eyed beans, lentils, or chickpeas), or positive control diet containing inulin (3). Fecal samples were collected at the end of each treatment (3). After DNA collection from the fecal samples, the V4 region of the 16S rRNA gene was amplified to produce 91 samples (3). For our analysis, we excluded the positive control diet samples, for a total of 63 mice RS samples and 14 mice control samples.

Preliminary metadata manipulation. Using R (v4.3.3; 7), with packages tidyverse (v2.0.0; 8) and readxl (v1.4.3; 9), the metadata from the Hughes et al. human dataset was filtered for timepoints 2 and 4 which correspond to samples which were collected after each treatment, while the metadata from the Kadyan et al. mice dataset was filtered to exclude the positive control inulin samples. They were then merged into a single metadata and a new category, "Group", was created to bin each of the samples into one of 4 groups: "human-C", "human-RS", "mouse-C", and "mouse-RS" for downstream analysis.

Data processing using the QIIME2 pipeline. Using Quantitative Insights Into Microbial Ecology 2 (QIIME2, v2024.2.0; 10), the human and mouse datasets were imported and demultiplexed. The datasets were denoised separately with Divisive Amplicon Denoising Algorithm 2 (DADA2) at a truncation length of 260 nucleotides to retain a median Phred Quality Score of 20 in the human dataset sequences (11). To maintain consistency, the truncation length of the mice dataset sequences was 260 nucleotides as well. The two datasets were then merged, followed by taxonomic classification on the merged dataset using the entire SILVA 138-99 classifier (12). Any mitochondrial or chloroplast DNA was filtered out. The outputs generated by QIIME2 processing on the merged dataset (ASV feature table, taxonomy table, and rooted phylogenetic tree) were then imported into R (7) for further processing.

Data processing using R. For the following step, the R packages ape (v5.7.1; 13), phyloseq (v1.46.0; 14), tidyverse (8), and vegan (v2.6.4; 15) are used. A phyloseq object was created in R (7) by integrating the outputs from the QIIME2 pipeline and the merged metadata.

Alpha and beta diversity analyses. To investigate the differences in gut microbiome diversity within and between our four groups ("human-C", "human-RS", "mouse-C", "mouse-RS"), we calculated the alpha and beta diversity. First, the phyloseq object previously

generated was filtered to remove any samples with less than 300 reads, before rarefying the samples at a sampling depth of 6747 to retain at least 10 samples each in the four groups we will be comparing. The R packages phyloseq (14), ape (13), tidyverse (8), picante (v1.8.2; 16), ARTool (v0.11.1; 17), ggsignif (v0.6.4; 18), pairwiseAdonis (v0.4; 19), and ggpubr (v0.6.0; 20) were used to generate the alpha and beta diversity metrics and the ggplot2 (v3.4.4; 21) package was used to visualize these metrics. All analyses were performed on the phyloseq object generated during data processing in R. A phyloseq wrapper function for richness from the phyloseq and vegan packages (14, 15) was used to determine Shannon's Diversity Index and Chao1, while the pd function from the picante package (16) was used to determine Faith's Phylogenetic Diversity. These three metrics used to quantify alpha diversity and each metric was visualized using a taxonomic boxplot. The Kruskal-Wallis test (alpha = 0.05) was applied to all three metrics to determine statistical significance in microbial diversity within the groups. For beta diversity analysis, the vegdist function in the vegan package (15) was used to determine Bray-Curtis dissimilarity. Bray-Curtis dissimilarly calculates the microbial diversity differences between the groups. A principal coordinate analysis (PCoA) plot was used to visualize the metric and statistical significance was calculated with permutational multivariate ANOVA (PERMANOVA) (alpha = 0.05) using the adonis2 function from the vegan package in R (15).

Core microbiome analysis. Core microbiome analysis was performed in R utilizing the packages tidyverse (8), phyloseq (14), and microbiome (v1.24.0; 22). The phyloseq object created during the data processing step was filtered by group, for a total of four groups: "human-C", "human-RS", "mouse-C", "mouse-RS". Core microbiome taxa were identified for all four groups at the genus and family level with a detection parameter of 0.001 (to filter out any rare ASVs) and a prevalence of 0.7 (present in 70% of samples). Core microbiome analyses were visualized with four-way Venn diagram comparisons using the package ggvenn (v0.1.10; 23).

Indicator species analysis. The indicator species analysis was run in R using the indicspecies (v1.7.14; 24), tidyverse (8), and phyloseq (14) at the genus and family level to identify key taxa among the four groups. The previously generated phyloseq object was converted to relative abundance, before using the multipatt function to cluster samples by group ("human-C", "human-RS", "mouse-C", "mouse-RS"). The taxonomy table was extracted from the relative abundance and merged with the phyloseq object, before filtering the results at $p < 0.05$. Following filtration, we kept only those that had an indicator species index value ≥ 0.8. Using ggplot2 (21), a bubble plot was constructed to visually compare prevalence and relative abundance of these key taxa across the groups.

Differential abundance analysis. Differential expression analysis based on the Negative Binomial distribution (DESeq) was done in R, utilizing the packages tidyverse (8), phyloseq (14), and DESeq2 (v1.42.1; 25). The phyloseq object previously generated was converted to a DESeq object, before running the DESeq function itself at the genus level. The results of the DESeq were used to generate comparisons between groups, namely: a "human-C" and "human-RS" comparison, a "mouse-C" and "mouse-RS" comparison, a "human-C" and "mouse-C" comparison, and a "human-RS" and "mouse-RS" comparison. Using the R package ggplot2 (21), these results were visualized as volcano plots with significantly differentially abundant taxa defined with an adjusted p-value of <0.01 and $|\log2FoldChange| > 2$.

Phylogenetic investigation of communities by reconstruction of unobserved states version 2.0 (PICRUSt2) analysis. To investigate if there were functional similarities between our groups, we ran a PICRUSt2 analysis. Using QIIME2 (10), the merged feature table file generated during the QIIME2 pipeline was filtered to remove any features with 5 or lower counts. Then, the QIIME2 PICRUSt2 plugin was used to generate a pathway abundance file as well as a KEGG orthology metagenome file. These files and the previously generated merged metadata were imported into R (9) for further analysis using the packages readr (v2.1.5; 26), ggpicrust2 (v1.7.3; 27), tibble (v3.2.1; 28), tidyverse (8), ggprism (v1.0.4; 29),

patchwork (v1.2.0; 30), DESeq2 (25), and ggh4x (v0.2.8; 31). Prior to running the differential abundance analysis, the abundance file was filtered to remove any pathways with less than 3 non-zero abundances, and the samples in abundance data were verified to match the samples in the metadata. Differential abundance analysis was done using the Linear Discriminant Analysis (LinDA) method (32) with Bonferroni p-value adjustment to compare the abundance of each pathway between the groups ("human-C", "human-RS", "mouse-C", "mouse-RS"). The pathways were annotated using the MetaCyc pathways database (33). Significant pathways were filtered for using an adjusted p-value of ≤ 0.05, while non-significant pathways were filtered for using an adjusted p-value of > 0.05. Using ggplot2 in R (21), principal component analysis (PCA) plots were used to visualize the significant and non-significant pathways between groups and a barplot was generated to compare the top abundant pathways from each group.

RESULTS

Microbial community richness and evenness were significantly different between resistant starch models. To determine differences in microbial community richness, evenness and phylogeny between the models, we measured Chao1, Shannon and Faith's phylogenetic diversity index for each dataset (Figure. 1). We found that richness was higher in human-C when compared to mouse-C, but there was no difference between the other groups, as well as no significant change in response to RS treatment (Figure. 1A). On the other hand, we found that Shannon's diversity index was significantly higher in the human groups than in the mouse groups, there was also a reduction in diversity after RS treatment in the human cohort, but no change in the mouse cohort (Figure. 1B). Finally, Faith's phylogenetic diversity was found to be similar across all groups with no statistically significant differences (Figure. 1C).

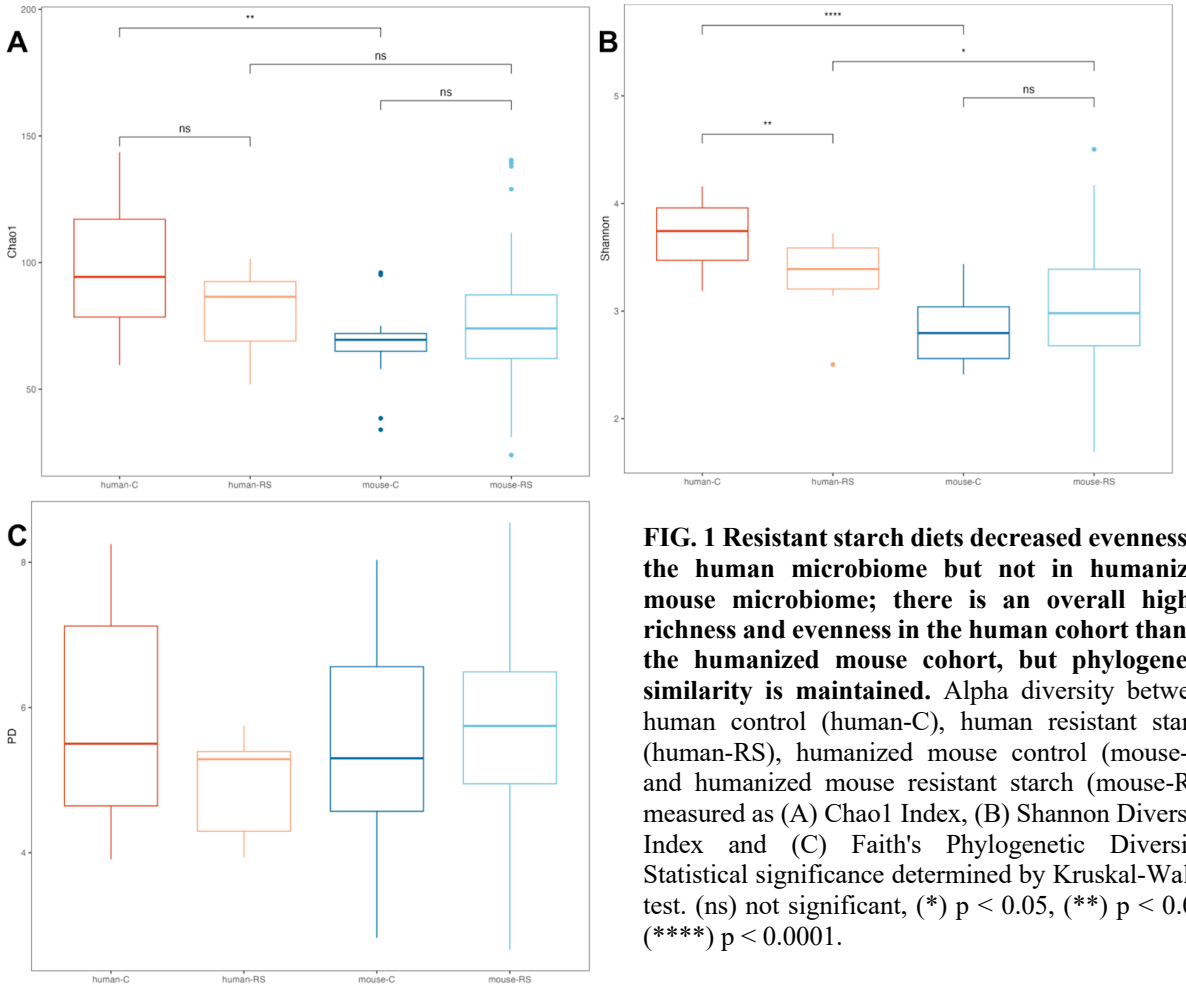

FIG. 1 Resistant starch diets decreased evenness in the human microbiome but not in humanized mouse microbiome; there is an overall higher richness and evenness in the human cohort than in the humanized mouse cohort, but phylogenetic similarity is maintained. Alpha diversity between human control (human-C), human resistant starch (human-RS), humanized mouse control (mouse-C) and humanized mouse resistant starch (mouse-RS) measured as (A) Chao1 Index, (B) Shannon Diversity Index and (C) Faith's Phylogenetic Diversity. Statistical significance determined by Kruskal-Wallis test. (ns) not significant, (*) $p < 0.05$, (**) $p < 0.01$, (****) $p < 0.0001$.

Microbial community structure differences were driven by species. To compare the human and humanized mice microbial communities, a beta diversity analysis was done using the Bray-Curtis dissimilarity metric. Microbial community structure was found to be significantly different between the human groups and mouse groups (R2 = 0.25, F = 10.975) (Figure 2). However, within each cohort the resistant starch status did not drive significant differences.

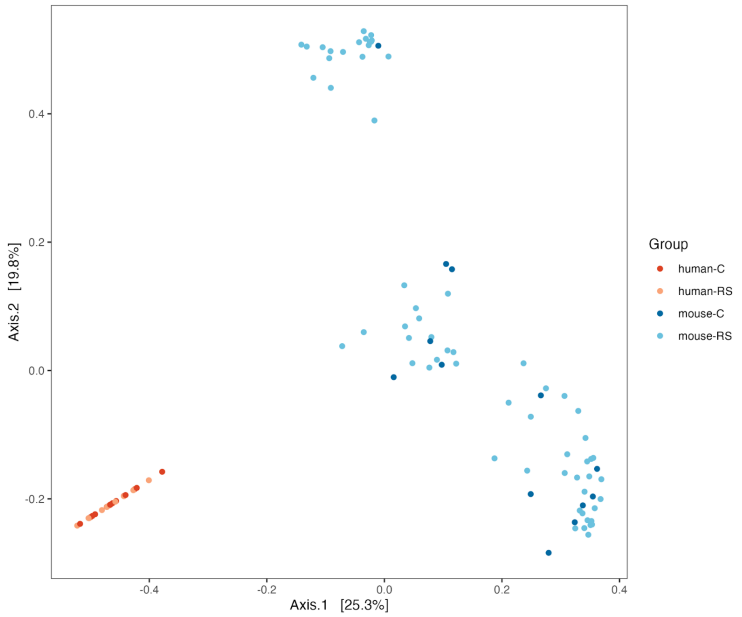

FIG. 2 Community structure differed by species but not treatment. Principal Coordinate Analysis plot (PCoA) of Bray-Curtis distance matrix between human-C, human-RS, mouse-C and mouse-RS. Statistical significance determined by PERMANOVA ($p < 0.001$).

Differential abundance analysis reveals significant differences in ASV abundance between RS human and humanized mice microbiomes. Differential abundance analysis was conducted to determine changes in ASV abundance between each of the four groups (human-C, human-RS, mouse-C, mouse-RS). Volcano plots were constructed to visualize these changes (Figure 3). The human microbial communities displayed fewer differentially

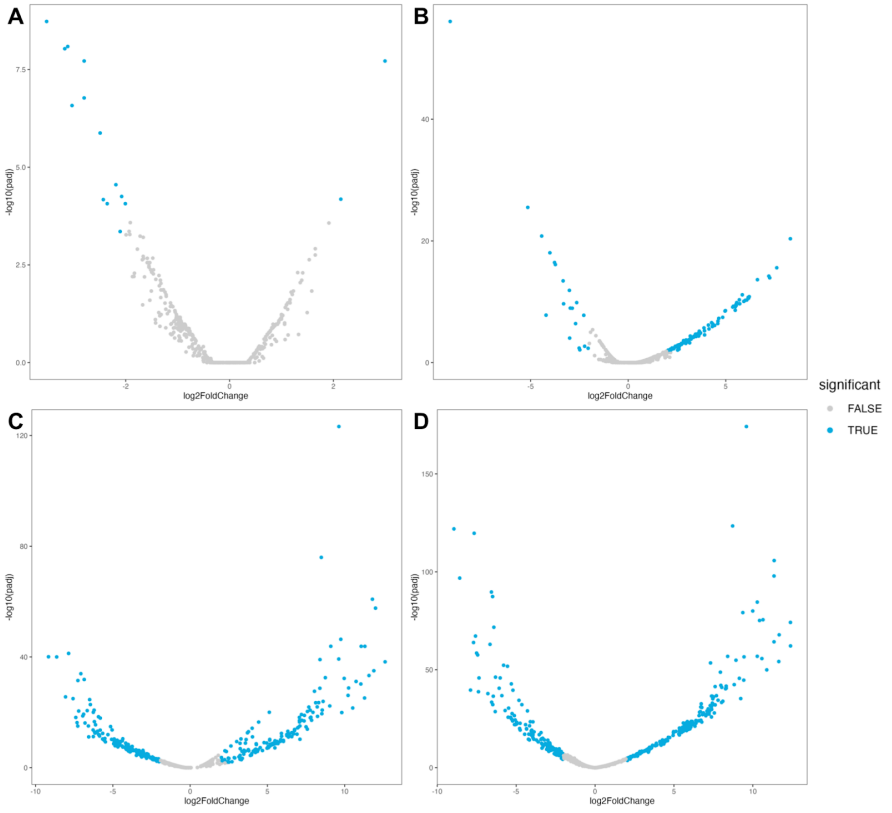

FIG. 3 Resistant starch diets affect ASV abundance differently in human vs. humanized mouse microbiomes. Differential abundance analysis between human-C, human-RS, mouse-C, and mouse-RS. Volcano plot comparing (A) human-C and human-RS, (B) mouse-C and mouse-RS, (C) human-C and mouse-C, and (D) human-RS and mouse-RS at an adjusted p-value cutoff of 0.01 and |log2FoldChange| > 2.

abundant ASVs in response to a RS diet when compared with the mouse microbial communities (Figure 3A & B). However, the responses to the diets showed different trends between the human and humanized mouse cohorts, with more downregulation of ASVs in the human microbiome (Figure 3A) and more upregulation of ASVs in the mouse microbiome (Figure 3B). Within the control groups, there were 305 differentially abundant ASVs in the mouse-C samples when compared to the human-C out of a total 2216 ASVs (Figure 3C). Within the RS groups, there were 363 differentially abundant ASVs in the mouse-RS samples when compared to the human-RS (Figure 3D).

Few key genera and core families shared between the models. We analysed core microbiome at genus and family level to identify shared taxa between the models. At a detection of 0.001 and prevalence of 70%, we found only 3 shared core genera between the four groups (Figure 4A): *Alistipes*, *Parabacteroides*, and *Bacteroides*; and the genus *Blautia*

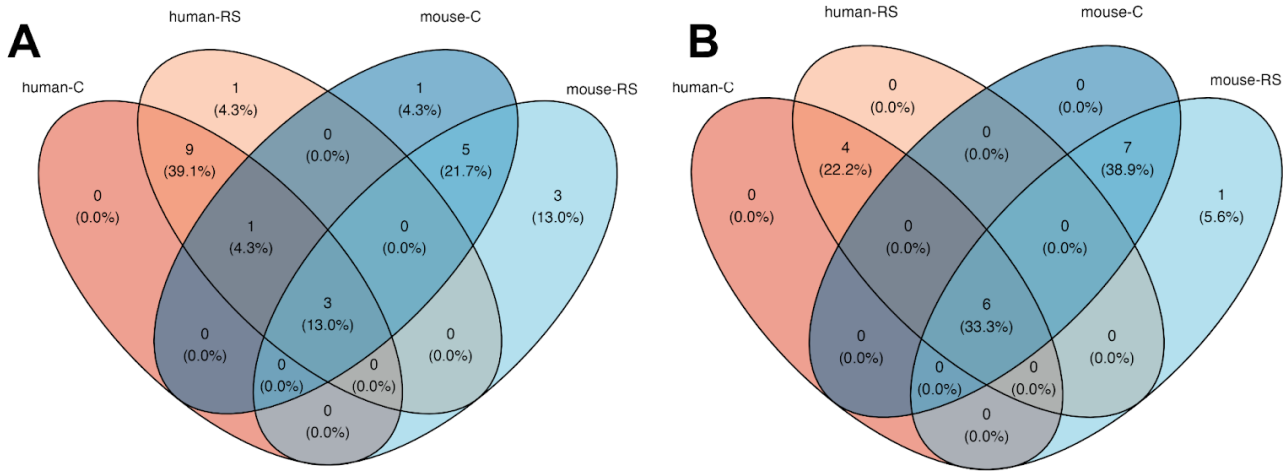

FIG. 4 More common taxa shared within than between the human and mouse cohorts. Core microbiome analysis at (A) Genus and (B) Family level between human-C, human-RS, mouse-C, and mouse-RS using detection value of 0.001 and prevalence of 0.7.

being shared among all except mouse-RS. The human model core genera found in both the control and RS groups were: *Bifidobacterium*, *Faecalibacterium*, *Subdoligranulum*, *Monoglobus*, *Dorea*, *Fusicatenibacter*, *Anaerostipes*, *Agathobacter*, and *[Eubacterium]_coprostanoligenes_group*. The only core genus found exclusively in human-RS is *Ruminococcus*. The core genera specific to the humanized mouse model were: *Akkermansia*, *Lactococcus*, *Streptococcus*, *Enterococcus*, and *Lachnoclostridium*. *Bilophila* was an exclusive core member of mouse-C; *Lactobacillus*, *Erysipelatoclostridium*, and *Colidextribacter* were exclusive to mouse-RS.

At the family taxonomic level we found 6 families that represent 33% of the core families being shared by all four groups (Figure 4B): *Bacteroidaceae*, *Ruminococcaceae*, *Oscillospiraceae*, *Lachnospiraceae*, *Rikenellaceae*, and *Tannerellaceae*. The 4 human specific families were: *Bifidobacteriaceae*, *Sutterellaceae*, *Monoglobaceae*, and *[Eubacterium]_coprostanoligenes_group* (of the order *Oscillospirales*). And the 7 core humanized mouse model families were: *Akkermansiaceae*, *Streptococcaceae*, *Desulfovibrionaceae*, *Enterococcaceae*, *Erysipelotrichaceae*, and *Erysipelatoclostridiaceae*. At this level only one family remained exclusive to one cohort-treatment group: *Lactobacillaceae* in the mouse-RS samples.

We ran an indicator species analysis at genus level to compare the abundance and prevalence of genera across the four groups (Figure S1). This analysis showed genera previously identified as core members such as *Akkermansia*, *Bifidobacterium*, and *Enterococcus*, but it also showed some genera not classified as core members: *Holdemania*, *Oscillospiraceae UCG-002*, *Lachnospiraceae_ND3007_group*, and *Lachnospiraceae_FCS020_group*. For a more stringent list of key genera associated with the groups we kept the matches in the core for each group and the indicator genera shown in Figure S1. While we found no indicator genus associated with all four groups, we found that *Bifidobacterium* (stat = 0.881) and *Anaerostipes* (stat = 0.872) were classified as indicator

genera for human-C, human-RS, and mouse-C even though they were classified as core members of the human samples only; *Streptococcus* (stat = 0.901) was classified as indicator for human-C, mouse-C, and mouse-RS; *Blautia* (stat = 0.975) was found to be both a core member and an indicator genera of the human-C, human-RS, and mouse-C groups. There were some human and humanized mouse exclusive key genera listed in Table 1, these are genera found in both the control and RS groups within each cohort.

TABLE. 1 Key genera specific to each cohort. The genera shown were chosen based on the union between core members as identified by the *core_members* function and the indicator taxa at a stat value >= 0.8 as identified by the *multipatt* function.

Human			
Family	**Genus**	**stat**	**p.value**
Ruminococcaceae	*Faecalibacterium*	0.983	0.005
	Subdoligranulum	0.966	0.005
[Eubacterium] coprostanoligenes group	*[Eubacterium] coprostanoligenes group*	0.814	0.005
Monoglobaceae	*Monoglobus*	0.895	0.005
Lachnospiraceae	*Dorea*	0.969	0.005
	Fusicatenibacter	0.965	0.005
	Agathobacter	0.957	0.005
Humanized mouse			
Akkermansiaceae	*Akkermansia*	0.868	0.005
Streptococcaceae	*Lactococcus*	0.991	0.005
Enterococcaceae	*Enterococcus*	1.000	0.005

Predicted microbial functions were significantly different between the human and humanized mouse microbiomes. We ran PICRUSt2 to estimate potential metabolic pathways associated with the ASVs. To compare the abundance of these pathways we ran a differential abundance analysis using the LinDA method between cohorts (human vs. humanized mouse). We found that 195 out of a total of 444 pathways were differentially expressed between humans and humanized mice, most of the pathways were not found to be significant. We compared the overall pathway composition between the groups (Figure 5A)

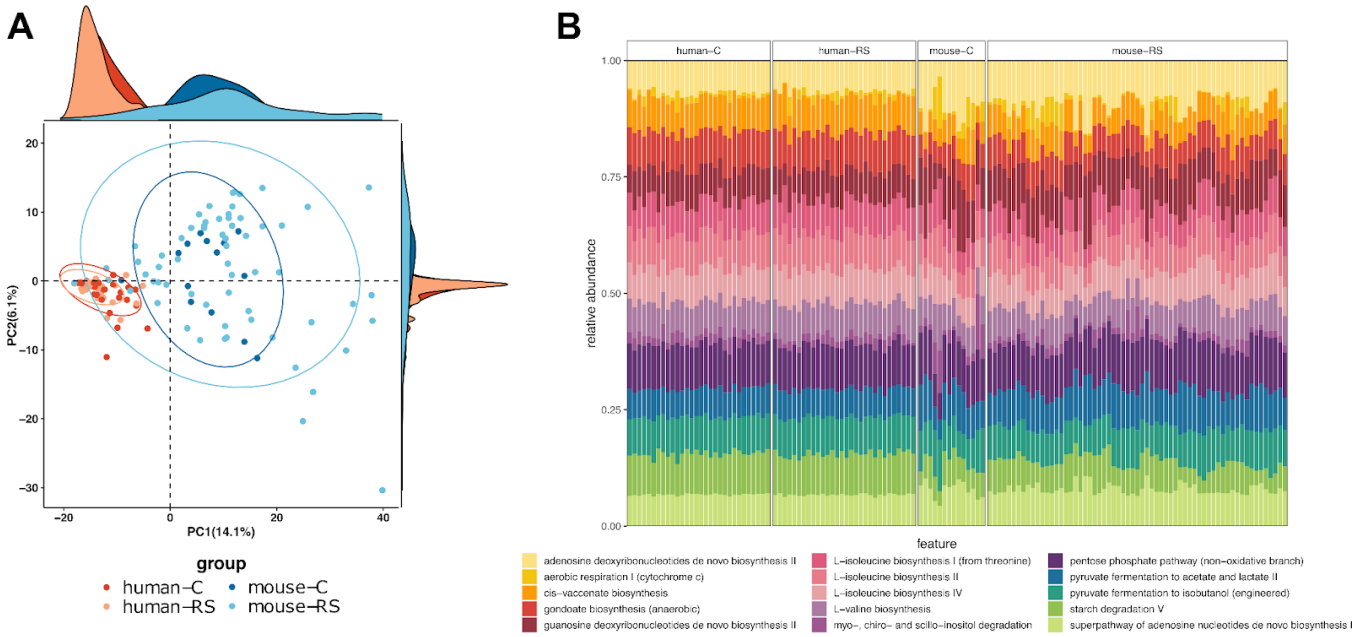

FIG. 5 Species drive estimated functional differences but not resistant starch diets. (A) Principal Component analysis (PCA) plot of predicted functional pathways of human-C, human-RS, mouse-C and mouse-RS microbiomes. (B) Barplot showing the relative abundance of the top 10 most abundant pathways from each group (15 pathways total) across all groups.

and found clear clusterings by models along the PC1 (14.1%) axis. We also determined the top 10 most abundant pathways in each group and compared the relative abundance across the samples in the four groups (Figure 5B). While all top pathways were present in both samples, there are some pathways that showed different abundances between cohorts, such as "starch degradation V" which would seem on average more abundant in the human samples than in the mouse samples. Overall, it would seem that the humanized mouse pathways hadmore variable abundance, this also relates to the increased dispersion shown in the PCA plot (Figure 5A). However statistical analysis would have to be carried out to quantify and test these differences.

DISCUSSION

Humanized mouse models have been identified as ideal models for conducting research related to the gut microbiome (34). In addition, diet has been shown to be a strong factor in shaping the gut microbiome in both humans and mice (35). This study looks at the mouse model used in Kadyan et al. compared to the human microbiome studied in Hughes et al. to determine if a mouse model is an acceptable model for determining the effects specifically of RS diets on the human microbiome. We hypothesized that humanized mice area good model for RS diets in humans and that it would play a similar role in shaping the microbial composition in both species due to a human microbiome in the mice model, resulting in a similar shift in taxa. We expected to find no significant differences between the cohorts across the comparisons and analysis made. Unfortunately, we found that the humanized mouse model used in this study is not an adequate model for studying the effects of RS diets when compared to the human RS diet study. Not only were there significant differences between the microbial compositions between humans and mice, but the microbial functions also differed significantly.

Based on the alpha diversity results, we see that there are no significant differences between the groups when comparing just richness or phylogenetic similarity. The differences observed seem to be mainly driven by abundance or evenness. The within species alpha diversity agree with what was observed in the original papers where significant differences were found in the human dataset but not the mouse dataset (2, 3). The unexpected alpha and beta diversity differences between species reveals distinct populations, which goes against our hypothesis.

The gut microbiome of humanized mice have previously been well established showing strong correlations between the donor human microbiome and the recipient mice microbiome (35). Interestingly, our alpha and beta diversity metrics suggest that the gut microbiome populations are significantly diverse from each other. Diet is known to be a strong determining factor for gut microbiome but even after a RS diet in both humans and mice, the microbial diversity still differs (34). In addition to diet, there are many other factors that could play a role in determining the composition of the gut microbiome (36). One possible explanation for the differences observed in diversity between humans and humanized mice before and after RS are the differing initial microbial communities because of the different individuals used to colonize the mice microbiome in Kadyan et al. and the participants in Hughes et al., as well as the different diets consumed by the subjects.

Following the diversity metric analysis, we wanted to determine if there are any compositional similarities by looking at taxa abundances or the presence of shared taxa using differential abundance, indicator taxa and core microbiome analysis. The differential abundance analysis revealed more taxonomic abundance differences before and after a RS diet between species, where humans showed 15 while mice showed 128 (Figure 3A and 3B). In addition, we also found that 305 taxa showed taxonomic abundance differences between control groups and 363 between RS groups, indicating significant differences in the abundance of taxa between the two species (Figure 3C and 3D). These results suggest that RS has varying effects on the two different microbiomes, causing more differential abundance changes in the humanized mice microbiome compared to the human as well as significantly higher differences in abundance before and after RS diets between the two groups. This may indicate that even before RS intervention there were already significant differences in abundance between the species' microbial composition.

Core microbiome analysis revealed more shared core genera within species, showing 9 between human-C and human-RS and 5 between mouse-C and mouse-RS, compared to only 3 between all groups. Interestingly, *Alistipes, Bacteroides*, *Parabacteroids*, found between all the groups are bacteria associated with carbohydrate metabolism and secretion of short chain fatty acids similar to the findings in both Kadyan et al. and Hughes et al. (2, 3, 37, 38). *Blautia*, found in all groups except mouse-RS, is also found to be associated with the production of SCFAs (39). Within the two species, almost all the core microbiome was found to be associated with SCFA secretion including *Bifidobacterium* found in human-C and human-RS and *Lachnoclostridium* found in mouse-C and mouse-RS (3, 40). When looking at the family level, we notice that the families like *Bacteroidaceae*, *Ruminococcaceae* and *Lachnospiraceae* were found to be common between all four groups, which are families associated with production of SCFA (41, 42, 43). Most of the microbial genus that were found to be distinct between the mice and humans belong to one of the 6 shared families that have been associated with the response to RS and secretion of SCFA.

After determining the core microbiome, we looked at the indicator taxa, looking specifically at the ASVs shared in the core microbiome analysis. Based on the combined results, human gut microbiomes are associated with more SCFA producing families including *Ruminocaccae, Monoglobacae and Lachnospiracae* (42, 43, 44). On the other hand, the humanized mouse microbiomes are also associated with SCFA producing families such as *Enterococceae,* but also non-SCFA producing bacteria like *Streptococcus,* which is known for their association with inflammation and infection response (45, 46). Human microbiomes show a stronger selection for SCFA producing bacteria compared with mice. Although mice and humans share biological similarities making them comparable to humans, there still exists anatomical differences between them such as the structure of the stomach, thickness of the colon and distribution of cell types throughout the digestive system (4). Due to these inherent differences, various taxa may not be capable of colonizing the gut microbiome from humans to mice, which could also affect the taxa that are capable of colonizing the gut microbiome (47). These differences between mice and humans could explain the slightly different core microbiome and indicator taxa as well as the differential abundances despite their seemingly overlapping functions based on compositional analysis.

Finally, we used PICRUSt2 to further investigate the functional profiles based on the differences found from the compositional analysis between mice and humans, in hopes of finding similarities. Functional analysis revealed overlapping functional profiles within species but the major pathways are similar between all groups, in addition 195 out of 444 pathways were found to be significantly different between the species. The shared major pathways between human and mice include core metabolic pathways such as the pentose phosphate pathway, adenosine deoxyribonucleotides de novo biosynthesis II and L-valine biosynthesis. These pathways are essential for the survival of organisms including nucleotide and amino acid synthesis (48, 49). This may suggest that non-essential pathways between the species are significantly different resulting in the differences between species.

Limitations Despite our results and analysis contradicting the predictions made in our study hypothesis, it is important to note the several limitations within our study. For example, one major limitation to consider was that both the human and mouse datasets exhibited significant variability in read lengths and quality, perhaps due to suboptimal sequencing conditions. Therefore, while truncating the mouse dataset to match the length of the human dataset, this may have oversimplified the mouse data and overlooked valuable information present in the full-length mouse sequences. As a result, this data could have been more comparable to the human cohort in downstream analysis.

Another major limitation to note was the sample size used in our study. Since there was a discrepancy in sample sizes between the human and mouse datasets, this can reduce the statistical power of the analysis and hinder our ability to identify potential subtle variations in the gut microbiome composition between human and mouse groups. In addition to the variable sample sizes, the datasets used small sample sizes, with 30 human-C and 30 human-RS samples, and 14 mouse-C and 63 mouse-RS samples. Consequently, the results generated may not be representative of the gut microbiome alterations in a broader human population in response to a RS-rich diet. Therefore, this limits the generalizability and applicability of

the conclusions made on how the mouse dataset is an inadequate model to translate findings of RS-rich diets effects on the human gut microbiome.

Another source of limitation was the differences in experimental methods between the mouse and human datasets. For instance, the RS diet exposure varied between the human and mouse groups; the mouse cohort strictly followed a 12-week diet intervention, whereas the human cohort participated in a cross-over study, with 1 week in a controlled or RS diet intervention, then 2-week washout, and lastly 1 week of the alternative diet. Therefore, not only was the study duration distinct between the mouse and human groups, but the administration and exposure of the RS diet varied as well, potentially affecting the results we generated. Moreover, since the datasets did not use the same exact RS-rich diets, other components of the administered diet could affect the gut microbiome response consequently. In the human dataset, participants were given RS2-enriched wheat rolls that provided roughly 14–19 g of resistant starch each day (2), whereas in the mouse dataset they were given various RS-rich beans (3); therefore, because there were no distinctions in the RS type and abundance used in each diet, the different levels of RS consumed could potentially play a role in the differences we observed in the gut microbiome response between the human and mouse groups. As a result, the methodological variability between the two datasets may be an influencing factor as to why the mouse model did not show similar gut microbial composition or functional alterations in response to a RS diet when compared with the given human dataset. In addition, developing the humanized mice with the pooled fecal content of only 5 healthy individuals may not fully capture the diversity and complexity of the human gut microbiome and could lead to biases in the microbial composition of the humanized mice when comparing the gut microbial effects of a RS diet in the human cohort. Overall, addressing and controlling for these limitations in future research will ameliorate our understanding of translational relevance of mouse model findings to human gut microbiome research.

Conclusions This study compares the effects of a RS diet on the gut microbiome composition and function between a humanized mouse model by Kadyan et al. (2023) (3) and human model by Hughes et al. (2021) (2) in order to assess the suitability of this mouse model for comparative analysis with humans. We found that there were significant differences between all four species-treatment groups except mouse control and mouse RS diet through Shannon diversity metrics, whereas in Faith's Phylogenetic diversity we found no significant differences between the four groups suggesting alpha diversity differences are driven mostly by abundance and not phylogenetic similarity. In the beta diversity analysis, we used Bray-Curtis dissimilarity to generate a principal coordinate analysis plot, revealing a significant separation between the four species-treatment groups and illustrates that the microbial community structure was significantly different between the human and mouse groups. Further analysis using the core microbiome showed few shared taxa among all 4 groups, also indicating notable microbial differences between the mouse and human cohorts. Likewise, differential abundance analysis comparing human and mouse control with human and mouse RS groups also illustrated significant differences between the mouse and human groups. Consequently, despite the compositional differences observed, PICRUSt2 analysis was done to investigate whether microbial functions were maintained between the mouse and human datasets. Upon generating the principal component analysis, the functions cluster together by mouse group and human group respectively, indicating that microbiome functions are different between mouse and human. Our findings ultimately suggest that the humanized mouse model by Kadyan et al. (2023) (3) is not an adequate model to compare the effects of a RS diet on the gut microbiome response with the human model by Hughes et al. (2021) (2). These findings thus emphasize the importance of cautious interpretation and further investigation when extrapolating results from animal models to human health research.

Future Directions To better understand the translatability of mouse models in the context of RS- rich diets in humans, future research can focus on compiling additional human and humanized mouse datasets to ensure a more comprehensive comparative analysis. When selecting potential mouse datasets, it is important to consider studies that use various diverse and representative pools of fecal donors to generate humanized mouse models. In addition,

because the datasets used different RS-rich diets, future research can implement a standardized protocol, such as using the same diet or directly transferring fecal samples from the humans being studied to the humanized mice. By matching the conditions in both species, this can lead to a stronger focus on the implications of a specific RS-rich diet, and can differentiate between the effects of the four distinct RS types on the gut microbiome respectively.

Using these two datasets, future studies can examine and compare the metabolites released in response to the RS diet in both the human and mouse groups. This approach may provide valuable insights into whether the mouse model shares similar metabolic activities of the gut microbiome in the context of human dietary interventions. Furthermore, exploring alternative models mentioned previously such as pigs, rats, and dogs is a promising area of research to determine whether there is a gut microbiome difference across species or if there are better species to model the effects of RS-rich diets in humans. In addition, further research evaluating the genetic and anatomical differences between mice and humans is vital in order to better reassess mouse models as a useful comparative tool for human gut microbiome research. Additionally, although this study focused on a more narrow time frame, looking at gut microbiome changes in weeks, future studies can examine longitudinal studies to help determine if the differences observed in the gut microbiome between humans and mice persists after longer periods on a RS diet. Lastly, additional studies can compare the changes of the gut microbiome in RS diets administered to humans and mice in both healthy and diseased states, such as diabetes and IBD, where RS diets are suggested to improve resilience to such chronic diseases (2). Collecting and analyzing more data from various human and mouse samples will ultimately provide greater insight into the dynamics of microbial community shifts over time, and can reveal similar or distinct patterns of adaptation or resilience between mice and humans to dietary interventions such as RS-rich diets.

DATA AVAILABILITY

The mouse dataset can be accessed via the National Library of Medicine (NIH) under accession number PMC7922998, and the human dataset can be found under accession number PMC10310774. Scripts used in QIIME2 and RStudio analysis are available at https://github.com/almita/micb475-team9/tree/main/data

ACKNOWLEDGEMENTS

We would like to thank Dr. Evelyn Sun, Bessie Wang, and the entire MICB 475 teaching team for their valuable mentorship and support during this project. Additionally, we extend our thanks to the UBC Department of Microbiology and Immunology for their funding and provision of resources. We also express our appreciation and gratitude to Hughes et al. and Kadyan et al. for generously providing the datasets used in our study.

CONTRIBUTIONS

AG: Carried out the data wrangling and guided the QIIME2 pipeline scripts. Carried out alpha and beta diversity analysis, contributed to the core microbiome analysis, carried out the indicator species analysis, and ran the PICRUSt2 analysis in R. Constructed the figures in R, and wrote the results section of the manuscript. Edited overall manuscript.
VH: Carried out Differential abundance analysis. Contributed to writing the discussion and figure legends. Edited overall manuscript.
LS: Carried out core microbiome analysis, QIIME2 processing of PICRUSt2 analysis, and contributed to the indicator species analysis. Wrote and refined abstract, study limitations, conclusions, and future directions. Edited overall manuscript.
GS: Carried out the core microbiome analysis, QIIME2 processing of PICRUSt2 analysis, and contributed to the indicator species analysis. Contributed to writing the methods section and editing the overall manuscript.
KS: Contributed to differential abundance analysis. Wrote the introduction section and contributed to overall editing of the manuscript.

REFERENCES

1. **Bendiks, Z. A., Knudsen, K. E. B., Keenan, M. J., & Marco, M. L.** 2020. Conserved and variable responses of the gut microbiome to resistant starch type 2. *Nutrition Research* **77**:12–28.
2. **Hughes, R. L., Horn, W. H., Finnegan, P., Newman, J. W., Marco, M. L., Keim, N. L., & Kable, M. E.** 2021. Resistant Starch Type 2 from Wheat Reduces Postprandial Glycemic Response with Concurrent Alterations in Gut Microbiota Composition. *Nutrients* **13**:645.
3. **Kadyan, S., Park, G., Wang, B., Singh, P., Arjmandi, B., & Nagpal, R.** 2023. Resistant starches from dietary pulses modulate the gut metabolome in association with microbiome in a humanized murine model of ageing. *Scientific Reports* **13**:10566.
4. **Nguyen, T. L., Vieira-Silva, S., Liston, A., & Raes, J.** (2015). How informative is the mouse for human gut microbiota research? *Disease Models & Mechanisms* **8**:1–16.
5. **Topping, D. L., & Clifton, P. M.** 2001. Short-chain fatty acids and human colonic function: roles of resistant starch and nonstarch polysaccharides. *Physiological reviews* **81**:1031–1064.
6. **Uhl, E. W., & Warner, N. J.** 2015. Mouse Models as Predictors of Human Responses: Evolutionary Medicine. *Current pathobiology reports* **3:**219–223.
7. **R Core Team**. 2023. R: A Language and Environment for Statistical Computing. *R Foundation for Statistical Computing, Vienna, Austria*. https://www.R-project.org/.
8. **Wickham H, Averick M, Bryan J, Chang W, McGowan LD, François R, Grolemund G, Hayes A, Henry L, Hester J, Kuhn M, Pedersen TL, Miller E, Bache SM, Müller K, Ooms J, Robinson D, Seidel DP, Spinu V, Takahashi K, Vaughan D, Wilke C, Woo K, Yutani H**. 2019. Welcome to the Tidyverse. *Journal of Open Source Software* **4**:1686.
9. **Wickham H, Bryan J.** 2023. Readxl: Read Excel Files. R package version 1.4.3, https://CRAN.R-project.org/package=readxl.
10. **Bolyen E, Rideout JR, Dillon MR, Bokulich NA, Abnet CC, Al-Ghalith GA, Alexander H, Alm EJ, Arumugam M, Asnicar F, Bai Y, Bisanz JE, Bittinger K, Brejnrod A, Brislawn CJ, Brown CT, Callahan BJ, Caraballo-Rodríguez AM, Chase J, Cope EK, Da Silva R, Diener C, Dorrestein PC, Douglas GM, Durall DM, Duvallet C, Edwardson CF, Ernst M, Estaki M, Fouquier J, Gauglitz JM, Gibbons SM, Gibson DL, Gonzalez A, Gorlick K, Guo J, Hillmann B, Holmes S, Holste H, Huttenhower C, Huttley GA, Janssen S, Jarmusch AK, Jiang L, Kaehler BD, Kang KB, Keefe CR, Keim P, Kelley ST, Knights D, Koester I, Kosciolek T, Kreps J, Langille MGI, Lee J, Ley R, Liu YX, Loftfield E, Lozupone C, Maher M, Marotz C, Martin BD, McDonald D, McIver LJ, Melnik AV, Metcalf JL, Morgan SC, Morton JT, Naimey AT, Navas-Molina JA, Nothias LF, Orchanian SB, Pearson T, Peoples SL, Petras D, Preuss ML, Pruesse E, Rasmussen LB, Rivers A, Robeson MS, Rosenthal P, Segata N, Shaffer M, Shiffer A, Sinha R, Song SJ, Spear JR, Swafford AD, Thompson LR, Torres PJ, Trinh P, Tripathi A, Turnbaugh PJ, Ul-Hasan S, van der Hooft JJJ, Vargas F, Vázquez-Baeza Y, Vogtmann E, von Hippel M, Walters W, Wan Y, Wang M, Warren J, Weber KC, Williamson CHD, Willis AD, Xu ZZ, Zaneveld JR, Zhang Y, Zhu Q, Knight R, and Caporaso JG.** 2019. Reproducible, interactive, scalable, and extensible microbiome data science using QIIME 2. *Nature Biotechnology* **37**: 852–857. https://doi.org/10.1038/s41587-019-0209-9
11. **Callahan BJ, McMurdie PJ, Rosen MJ, Han AW, Johnson AJA, Holmes SP.** 2016. DADA2: High- resolution sample inference from Illumina amplicon data. *Nat Methods* **13**:581–583
12. **Quast C, Pruesse E, Yilmaz P, Gerken J, Schweer T, Yarza P, Peplies J, Glöckner FO**. 2013. The SILVA ribosomal RNA gene database project: improved data processing and web-based tools. *Nucl Acids Res.* **41**:D590-D596.
13. **Paradis E, Schliep K**. 2019. ape 5.0: an environment for modern phylogenetics and evolutionary analyses in R. *Bioinformatics*. **35**:526-528. doi:10.1093/bioinformatics/bty633
14. **McMurdie PJ, Holmes S**. 2013. phyloseq: An R package for reproducible interactive analysis and graphics of microbiome census data. *PLoS ONE* ***8*(4)**:e61217. http://dx.plos.org/10.1371/journal.pone.0061217
15. **Oksanen J, Simpson G, Blanchet F, Kindt R, Legendre P, Minchin P, O'Hara R, Solymos P, Stevens M, Szoecs E, Wagner H, Barbour M, Bedward M, Bolker B, Borcard D, Carvalho G, Chirico M, De Caceres M, Durand S, Evangelista H, FitzJohn R, Friendly M, Furneaux B, Hannigan G, Hill M, Lahti L, McGlinn D, Ouellette M, Ribeiro Cunha E, Smith T, Stier A, Ter Braak C, Weedon J.** 2022. vegan: Community Ecology Package. R package version 2.6-4, https://CRAN.R-project.org/package=vegan
16. **Kembel SW, Cowan PD, Helmus MR, Cornwell WK, Morlon H, Ackerly DD, Blomberg SP, Webb CO**. 2010. picante: R tools for integrating phylogenies and ecology. *Bioinformatics* **26**:1463-1464.
17. **Kay M, Elkin L, Higgins J, Wobbrock J.** 2021. ARTool: Aligned Rank Transform for Nonparametric Factorial ANOVAs. R package version 0.11.1. doi:10.5281/zenodo.594511, https://github.com/mjskay/ARTool
18. **Ahlmann-Eltze, C., & Patil, I**. 2021. ggsignif: R Package for Displaying Significance Brackets for 'ggplot2'. PsyArxiv. doi:10.31234/osf.io/7awm6
19. **Martinez Arbizu, P**. 2020. pairwiseAdonis: Pairwise multilevel comparison using adonis. R package version 0.4

20. **Kassambara, A**. 2022. Ggpubr: 'Ggplot2' Based Publication Ready Plots. https://cran.r-project.org/web/packages/ggpubr/index.html
21. **Wickham, H**. 2016. ggplot2: Elegant Graphics for Data Analysis. *Springer-Verlag* New York.
22. **Lahti L & Shetty S**. 2012. Microbiome R package. R package version 1.24.0. http://microbiome.github.io
23. **Yan L.** 2023. ggvenn: Draw Venn Diagram by 'ggplot2'. R package version 0.1.10, https://CRAN.R-project.org/package=ggvenn.
24. **De Cáceres M, Legendre P**. 2009. Associations between species and groups of sites: indices and statistical inference. *Ecology*. **90**:3566-3574.
25. **Love MI, Huber W, Anders S**. 2014. Moderated estimation of fold change and dispersion for RNA-seq data with DESeq2. *Genome Biology.* ***15***:550
26. **Wickham H, Hester J, Bryan J**. 2024. readr: Read Rectangular Text Data. R package version 2.1.5, https://CRAN.R-project.org/package=readr.
27. **Yang C, Mai J, Cao X, Burberry A, Cominelli F, Zhang L.** 2023. ggpicrust2: an R package for PICRUSt2 predicted functional profile analysis and visualization. *Bioinformatics.* ***39*****(8)**:btad470. https://doi.org/10.1093/bioinformatics/btad470
28. **Müller K, Wickham H.** 2023. tibble: Simple Data Frames. R package version 3.2.1, https://CRAN.R-project.org/package=tibble.
29. **Dawson C.** 2022. ggprism: A 'ggplot2' Extension Inspired by 'GraphPad Prism'. R package version 1.0.4, https://CRAN.R-project.org/package=ggprism.
30. **Pedersen T.** 2024. patchwork: The Composer of Plots. R package version 1.2.0, https://CRAN.R-project.org/package=patchwork.
31. **van den Brand T.** 2024. ggh4x: Hacks for 'ggplot2'. R package version 0.2.8, https://CRAN.R-project.org/package=ggh4x.
32. **Liu ZP.** 2013. Linear Discriminant Analysis. *In: Dubitzky, W., Wolkenhauer, O., Cho, KH., Yokota, H. (eds) Encyclopedia of Systems Biology*. Springer, New York, NY. https://doi.org/10.1007/978-1-4419-9863-7_395
33. **Caspi R, Altman T, Billington R, Dreher K, Foerster H, Fulcher CA, Holland TA, Keseler IM, Kothari A, Kubo A, Krummenacker M, Latendresse M, Mueller LA, Ong Q, Paley S, Subhraveti P, Weaver DS, Weerasinghe D, Zhang P, Karp PD.** 2014. The MetaCyc Database of metabolic pathways and enzymes and the BioCyc collection of Pathway/Genome Databases. *Nucleic Acids Research* **42**:D459-D471.
34. **Bokoliya SC, Dorsett Y, Panier H, Zhou Y.** 2021**.** Procedures for fecal microbiota transplantation in murine microbiome studies. *Frontiers in Cellular and Infection Microbiology* **11**:711055.
35. **Park JC, Im S-H.** 2020**.** Of men in mice: The development and application of a humanized gnotobiotic mouse model for microbiome therapeutics. *Experimental & Molecular Medicine* **52**:1383–1396.
36. **Wen L, Duffy A.** 2017**.** Factors influencing the gut microbiota, inflammation, and type 2 diabetes. *The Journal of Nutrition* **147**:7.
37. **Parker BJ, Wearsch PA, Veloo AC, Rodriguez-Palacios A.** 2020**.** The genus *Alistipes*: Gut bacteria with emerging implications to inflammation, cancer, and mental health. *Frontiers in Immunology* **11**:906.
38. **Cui Y, Zhang L, Wang X, Yi Y, Shan Y, Liu B, Zhou Y, Lü X.** 2022**.** Roles of intestinal *Parabacteroides* in human health and diseases. FEMS Microbiology Letters **369.**
39. **Liu X, Mao B, Gu J, Wu J, Cui S, Wang G, Zhao J, Zhang H, Chen W.** 2021**.** blautia—a new functional genus with potential probiotic properties? *Gut Microbes* **13:**1875796.
40. **Zhang Y-J, Li S, Gan R-Y, Zhou T, Xu D-P, Li H-B.** 2015. Impacts of gut bacteria on human health and diseases. *International Journal of Molecular Sciences* **16**:7493–7519.
41. **Amini Khiabani S, Haghighat S, Tayebi Khosroshahi H, Asgharzadeh M, Samadi Kafil H.** 2023. Diversity of *Bacteroidaceae* family in gut microbiota of patients with chronic kidney disease and end stage renal disease. *Health Promotion Perspectives* **13**:237–242.
42. **Gu X, Sim JXY, Lee WL, Cui L, Chan YFZ, Chang ED, Teh YE, Zhang A-N, Armas F, Chandra F, Chen H, Zhao S, Lee Z, Thompson JR, Ooi EE, Low JG, Alm EJ, Kalimuddin S.** 2022. Gut *Ruminococcaceae* levels at baseline correlate with risk of antibiotic-associated diarrhea. *iScience* **25:**103644**.**
43. **Dandachi I, Anani H, Hadjadj L, Brahimi S, Lagier J-C, Daoud Z, Rolain J-M.** 2021. Genome analysis of *Lachnoclostridium phocaeense* isolated from a patient after kidney transplantation in Marseille. *New Microbes and New Infections* **41**:100863.
44. **Wang L, Wu D, Zhang Y, Li K, Wang M, Ma J.** 2023. Dynamic distribution of gut microbiota in cattle at different breeds and health states. *Frontiers in Microbiology* **14**:1113730.
45. **Baldelli V, Scaldaferri F, Putignani L, Del Chierico F.** 2021. The role of *Enterobacteriaceae* in gut microbiota dysbiosis in inflammatory bowel diseases. *Microorganisms* **9**:697.
46. **Sayols-Baixeras S, Dekkers KF, Baldanzi G, Jönsson D, Hammar U, Lin Y-T, Ahmad S, Nguyen D, Varotsis G, Pita S, Nielsen N, Eklund AC, Holm JB, Nielsen HB, Ericson U, Brunkwall L, Ottosson F, Larsson A, Ericson D, Klinge B, Nilsson PM, Malinovschi A, Lind L, Bergström G, Sundström J, Ärnlöv J, Engström G, Smith JG, Orho-Melander M, Fall T.** 2022. *Streptococcus* Species Abundance in the Gut Is Linked to Subclinical Coronary Atherosclerosis in 8973 Participants From the SCAPIS Cohort. *Circulation* **148**:459–472.

47. **Walter J, Armet AM, Finlay BB, Shanahan F.** 2020. Establishing or exaggerating causality for the gut microbiome: Lessons from human microbiota-associated rodents. *Cell* **180**:221–232.
48. **Maruyama A, Sato Y, Nakayama J, Murai J, Ishikawa T, Soga T, Makinoshima H.** 2021. De novo deoxyribonucleotide biosynthesis regulates cell growth and tumor progression in small-cell lung carcinoma. *Sci Rep* **11**:13474.
49. **Amorim Franco TM, Blanchard JS.** 2017. Bacterial branched-chain amino acid biosynthesis: structures, mechanisms, and drugability. *Biochemistry* **56**:5849–5865.